Journal of Sound and Vibration (2001) **240**(1), 159–182
doi:10.1006/jsvi.2000.3197, available online at http://www.idealibrary.com on IDEAL®

TORSIONAL VIBRATION ANALYSIS OF GEAR-BRANCHED SYSTEMS BY FINITE ELEMENT METHOD

J.-S. Wu and C.-H. Chen

Institute of Naval Architecture and Marine Engineering, National Cheng-Kung University, Tainan, Taiwan 701, *Republic of China. E-mail: jswu@mail.ncku.edu.tw*

(*Received* 3 *April* 2000, *and in final form* 12 *July* 2000)

The purpose of this paper is to present a simple approach for eliminating the "dependent" torsional angles existing in the reduction gears of a gear-branched system so that this system may be modelled as an equivalent straight-geared (or direct-transmitted) system. Then the overall mass matrix, damping matrix, stiffness matrix, and load vector of the direct-transmitted system are obtained with the conventional finite element method (FEM) by assembling the elemental property matrices of all the shaft elements contained in the torsional system. Based on the overall property matrices determined, the equations of motion of the whole vibrating system are defined. Solution of the equations of motion gives the dynamic responses and solution of the associated eigenvalue equation provides the natural frequencies and the mode shapes of the system. A simple technique is also presented to study the influence of the shaft mass on the natural frequencies of a torsional system.

1. INTRODUCTION

In the early years, the torsional vibration analysis of a "straight-geared" (or direct-transmitted) system was performed using the Holzer method [1], irrespective of whether the system was undamped [2, 3] or damped [4–6]. After the advent of computers, the more effective transfer matrix method was developed to solve the problem [7–9]. The torsional vibration of a "gear-branched" system (having reduction gears) has been solved with the system matrix eigenvalue extraction method or the trial- and-error search method based on the matrix transfer/Holzer procedures [10–13].

In recent years, the finite element method (FEM) has been used to do the torsional vibration analysis of a straight-geared system [14] and a gear-branched system [15, 16]. In general, the FEM formulation for a gear-branched system is much difficult than that of a straight-geared system. The difficulty arises from the fact that the total "independent" degrees of freedom (d.o.f.) of a gear-branched system (with rigid gears and rigid teeth) is less than the total number of rotating gears (or disks) because of the existence of the reduction gears between the adjacent branches. In reference [16], two rotating disks coupled by an elastic shaft segment are considered as a finite element. Based on this definition, the element stiffness matrix $[k_e]_i$ and element mass matrix $[m_e]_i$ are derived. Then the overall stiffness matrix $[k]$ and the overall mass matrix $[m]$ are obtained by assembling all the element matrices $[k_e]_i$ and $[m_e]_i$ respectively. In order to eliminate the "dependent" d.o.f., the transformations $[\bar{k}] = [T]^{\mathrm{T}}[k][T]$ and $[\bar{m}] = [T]^{\mathrm{T}}[m][T]$ are made. The matrix $[T]$ is

0022-460X/01/060159 + 24 $35.00/0

a $m \times n$ rectangular transformation matrix with coefficients being equal to 0, 1 or R_j, where $R_j\,(j = 1, 2, \ldots)$ is the transmission ratio of the jth reduction gear. Since the total number of rows of $[T]$, m, is equal to the "independent" total d.o.f. together with the "dependent" ones, and the total number of columns of $[T]$, n, is equal to the "independent" total d.o.f., it is evident that although $[k]$ and $[m]$ are the $m \times m$ square matrices, $[\bar{k}]$ and $[\bar{m}]$ are the $n \times n$ ones. From the foregoing description, one sees that the formulation of reference [16] cannot reveal the advantage of the FEM. For this reason, a simple approach is presented in this paper to eliminate the dependent torsional angles existing in the reduction gears, so that a gear-branched system may be modelled as an equivalent straight-geared (or direct-transmitted) system. Hence, the overall property matrices of the entire torsional system may be obtained with the conventional assembling technique of the FEM and no overall transformation or element-by-element transformations as adopted by references [15, 16] are required.

By using the presented approach, an equation of motion with the standard form will be easily obtained. After that, the simple Jacobi method [17] may be used to solve the undamped natural frequencies and the popular Newmark direct integration method [17] may be used to solve the forced vibration responses due to external excitations. It is worth mentioning that the presented approach is applicable to both undamped and damped systems.

2. DERIVATION OF PROPERTY MATRICES OF A SHAFT ELEMENT

Figure 1(a) shows one part of a gear-branched system, where shaft p and shaft q are connected by two gears with radii of pitch circles r_j and r'_j respectively. The equations of motion for the two-shaft elements are given by [15–17]

$$\begin{bmatrix} I_i + \frac{1}{3}I_p & \frac{1}{6}I_p \\ \frac{1}{6}I_p & I_j + \frac{1}{3}I_p \end{bmatrix} \begin{Bmatrix} \ddot{\theta}_i \\ \ddot{\theta}_j \end{Bmatrix} + \begin{bmatrix} c_i & 0 \\ 0 & c_j \end{bmatrix} \begin{Bmatrix} \dot{\theta}_i \\ \dot{\theta}_j \end{Bmatrix} + \begin{bmatrix} k_p & -k_p \\ -k_p & k_p \end{bmatrix} \begin{Bmatrix} \theta_i \\ \theta_j \end{Bmatrix} = \begin{Bmatrix} F_i \\ F_j \end{Bmatrix}, \tag{1}$$

$$\begin{bmatrix} I'_j + \frac{1}{3}I_q & \frac{1}{6}I_q \\ \frac{1}{6}I_q & I_k + \frac{1}{3}I_q \end{bmatrix} \begin{Bmatrix} \ddot{\theta}'_j \\ \ddot{\theta}_k \end{Bmatrix} + \begin{bmatrix} c'_j & 0 \\ 0 & c_k \end{bmatrix} \begin{Bmatrix} \dot{\theta}'_j \\ \dot{\theta}_k \end{Bmatrix} + \begin{bmatrix} k_q & -k_q \\ -k_q & k_q \end{bmatrix} \begin{Bmatrix} \theta'_j \\ \theta_k \end{Bmatrix} = \begin{Bmatrix} F'_j \\ F_k \end{Bmatrix}, \tag{2}$$

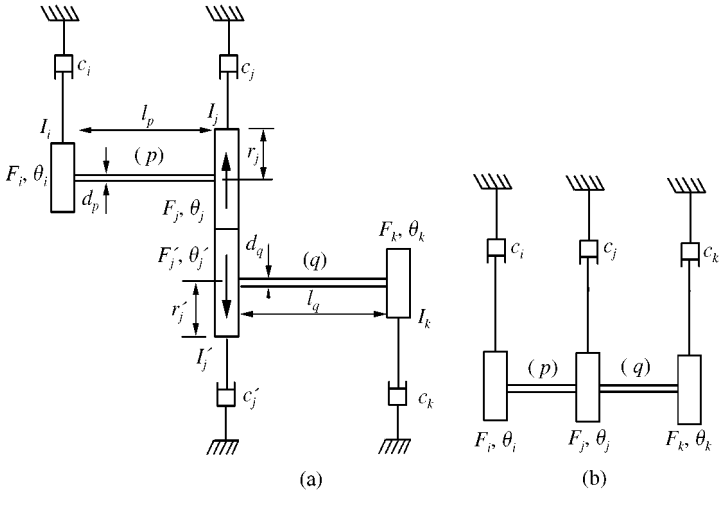

Figure 1. (a) Shafts p and q connected with reduction gears, (b) equivalent straight-geared system with no speed reduction.

where $I_p = \rho(\pi d_p^4/32)l_p$ and $k_p = G(\pi d_p^4/32)l_p$ are the polar mass moment of inertia and torsional spring constant of shaft p respectively. Furthermore, $\ddot{\theta}$, $\dot{\theta}$, and θ are the angular acceleration, velocity, and displacement, c is the damping coefficient, F is the external load, d and l are the diameter and length of shaft, while G and ρ are the shear modulus and mass density of the shaft material, respectively. The notations with subscripts i, j, j' and k, respectively, represent the associated parameters of gears i, j, j' and k. Similarly, those with subscripts p and q denote the associated parameters of shafts p and q respectively.

Compatibility of the angular displacements between the reduction gears j and j' requires that

$$r_j\theta_j = -r'_j\theta'_j \tag{3a}$$

or

$$\theta'_j = -\frac{r_j}{r'_j}\theta_j = -R_j\theta_j, \tag{3b}$$

where the negative sign denotes the direction of θ'_j being opposite to that of θ_j, while

$$R_j = r_j/r'_j. \tag{4}$$

Since r_j and r'_j are the radii of pitch circles of gears j and j', $R_j = r_j/r'_j$ represents the speed ratio of the driven shaft q to driving shaft p, or the gear ratio of master gear j to slave gear j'.

For convenience of derivation, the following equality equation is introduced:

$$\theta_k = \theta_k. \tag{5}$$

Writing equations (3b) and (5) in the matrix form gives

$$\{\theta'\} = [\lambda]\{\theta\}, \tag{6}$$

where

$$\{\theta'\} = \{\theta'_j \ \theta_k\}, \quad \{\theta\} = \{\theta_j \ \theta_k\}, \quad [\lambda] = \begin{bmatrix} -R_j & 0 \\ 0 & 1 \end{bmatrix}. \tag{7a)–(7c)}$$

From equation (6) one has

$$\{\dot{\theta}'\} = [\lambda]\{\dot{\theta}\}, \quad \{\ddot{\theta}'\}[\lambda]\{\ddot{\theta}\} \tag{8a), (8b)}$$

where

$$\{\dot{\theta}'\} = \{\dot{\theta}'_j \ \dot{\theta}_k\}, \quad \{\dot{\theta}\} = \{\dot{\theta}_j \ \dot{\theta}_k\} \tag{9a), (9b)}$$

$$\{\ddot{\theta}'\} = \{\ddot{\theta}'_j \ \ddot{\theta}_k\}, \quad \{\ddot{\theta}\} = \{\ddot{\theta}_j \ \ddot{\theta}_k\}. \tag{10a), (10b)}$$

In the above equations, $\{\cdot\}$ represents a column vector and $[\lambda]$ is the transformation matrix for eliminating the "dependent" angular displacement θ'_j. Substituting equations (6), (8a) and (8b) into equation (2) and then premultiplying both sides of the resulting equation by $[\lambda]^T$, one obtains

$$[m_e]\{\ddot{\theta}\} + [c_e]\{\dot{\theta}\} + [k_e]\{\theta\} = \{f_e\}, \tag{11}$$

where

$$[m_e] = \begin{bmatrix} R_j^2(I'_j + \frac{1}{3}I_q) & -R_j(\frac{1}{6}I_q) \\ -R_j(\frac{1}{6}I_q) & I_k + \frac{1}{3}I_q \end{bmatrix}, \quad [c_e] = \begin{bmatrix} R_j^2 c'_j & 0 \\ 0 & c_k \end{bmatrix}, \quad [k_e] = \begin{bmatrix} R_j^2 k_q & R_j k_q \\ R_j k_q & k_q \end{bmatrix},$$

$$\{f_e\} = \begin{Bmatrix} -R_j F'_j \\ F_k \end{Bmatrix}. \tag{12a–d}$$

It is noted that the "dependent" angular displacement θ'_j is eliminated in equation (11). Also, the elemental mass matrix $[m_e]$, damping matrix $[c_e]$, stiffness matrix $[k_e]$, and the load vector $\{f_e\}$ of the "driven" shaft q, as defined by equations (12a)–(12d), will take the same forms as those of the "driving" shaft p (see equation (1)) if one sets $R_j = -1$. In other words, equations (12a)–(12d) are the key expressions of the presented approach, since one may use them to define the elemental property matrices of all the shaft elements composed of a gear-branched system. The only difference between the elemental property matrices for a "driving" shaft (with master gear) and those for a "driven" shaft (with slave gear) is that $R_j = -1$ for the former and $R_j = r_m/r_s$ for the latter, where r_m and r_s represent the radii of the pitch circles for the master gear and the slave gear respectively.

According to the conventional FEM, by assembling the associated elemental property matrices of the shaft elements p and q connected with the reduction gears as shown in Figure 1(a), one obtains the following equations of motion for the equivalent straight-geared system with no speed reduction as shown in Figure 1(b):

$$\begin{bmatrix} I_i + \frac{1}{3}I_p & \frac{1}{6}I_p & 0 \\ \frac{1}{6}I_p & (I_j + \frac{1}{3}I_p) + R_j^2(I'_j + \frac{1}{3}I_q) & -R_j(\frac{1}{6}I_q) \\ 0 & -R_j(\frac{1}{6}I_q) & I_k + \frac{1}{3}I_q \end{bmatrix} \begin{Bmatrix} \ddot{\theta}_i \\ \ddot{\theta}_j \\ \ddot{\theta}_k \end{Bmatrix}$$

$$+ \begin{bmatrix} c_i & 0 & 0 \\ 0 & c_j + R_j^2 c'_j & 0 \\ 0 & 0 & c_k \end{bmatrix} \begin{Bmatrix} \dot{\theta}_i \\ \dot{\theta}_j \\ \dot{\theta}_k \end{Bmatrix} + \begin{bmatrix} k_p & -k_p & 0 \\ -k_p & k_p + R_j^2 k_q & R_j k_q \\ 0 & R_j k_q & k_q \end{bmatrix} \begin{Bmatrix} \theta_i \\ \theta_j \\ \theta_k \end{Bmatrix} = \begin{Bmatrix} F_i \\ F_j - R_j F'_j \\ F_k \end{Bmatrix}. \tag{13}$$

From the above derivations one sees that any two shaft elements connected by a reduction-gear set as shown in Figure 1(a) may be replaced by an equivalent straight-geared (or direct-transmitted) system without the reduction gear as shown in Figure 1(b) so that the conventional assembling technique for the FEM is possible.

3. DETERMINATION OF AN EQUIVALENT DIRECT-TRANSMITTED SYSTEM FROM A GEAR-BRANCHED SYSTEM

Figure 2(a) shows the block diagram of a gear-branched system [2]. The labels (1)–(6) represent the numbering of the six shaft elements and 1–10 represent the 10 gears (or disks). Furthermore, R_2 and R_5 represent the speed ratios of shaft (2) and shaft (5) to shaft (1), respectively, and R_6 is the speed ratio of shaft (6) to shaft (5). It is noted that the digits with parentheses ( ) denote the numbering of the shafts and those without parentheses denote the numbering of the gears. Since the angular displacements of disks 3, 7, and 9 are dependent on those of disks 2 and 8, the numberings of disks 3, 7, and 9 as shown in

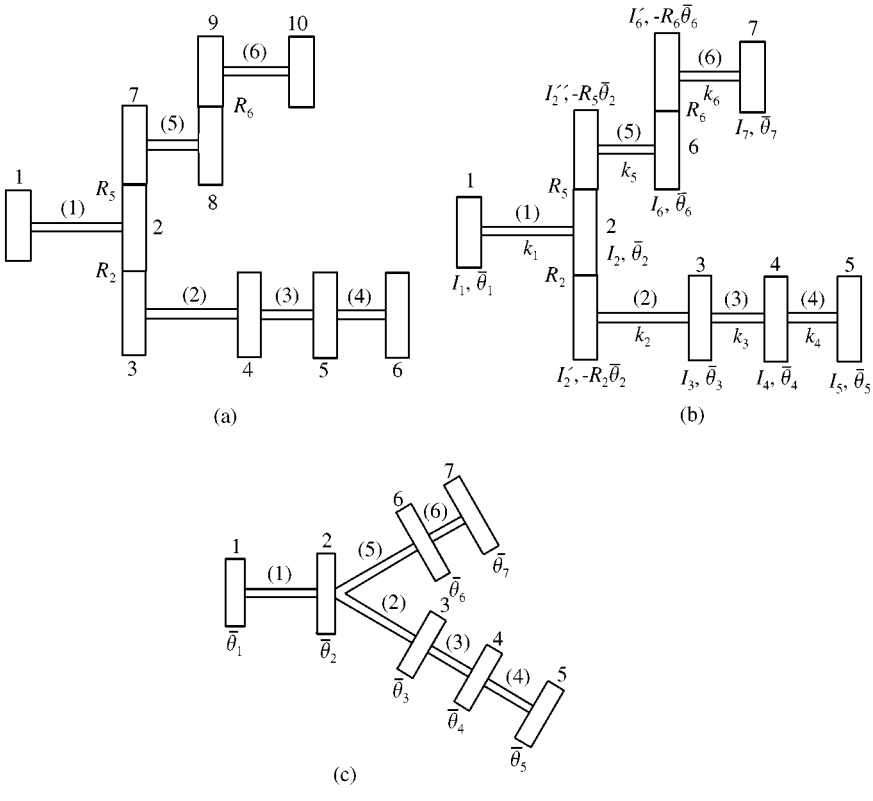

Figure 2. (a) The original gear-branched system [2]; (b) notations for the gear-branched system; and (c) the equivalent direct-transmitted gear system.

Figure 2(a) are eliminated in Figure 2(b), where the angular displacements of the three unnumbered disks are represented by $-R_2\bar{\theta}_2$, $-R_5\bar{\theta}_2$ and $-R_6\bar{\theta}_6$ respectively. In addition, the mass moments of inertia of the forgoing three disks are denoted by I_2', I_2'', and I_6', respectively, where the subscripts 2 and 6 are the identification numbers for the master gears with which the slave gears of the driven shafts (2), (5), and (6) are connected. Figure 2(c) represents the equivalent direct-transmitted system of the original gear-branched system shown in Figure 2(a). Based on the theory presented in the last section, the property matrices for each shaft element in the direct-transmitted gear system are listed below. For simplicity, the system is assumed to be undamped (i.e., $c_j \cong 0$) with negligible shaft mass ($\rho \cong 0$) and no excitations ($F_k = 0$, $k = 1$–7):

$$[m_e]_1 = \begin{matrix} \ddot{\bar{\theta}}_1 & \ddot{\bar{\theta}}_2 \end{matrix} \begin{bmatrix} I_1 & 0 \\ 0 & I_2 \end{bmatrix} \begin{matrix} \ddot{\bar{\theta}}_1, \\ \ddot{\bar{\theta}}_2 \end{matrix} \quad [k_e]_1 = \begin{matrix} \bar{\theta}_1 & \bar{\theta}_2 \end{matrix} \begin{bmatrix} k_1 & -k_1 \\ -k_1 & k_1 \end{bmatrix} \begin{matrix} \bar{\theta}_1 \\ \bar{\theta}_2 \end{matrix} \quad \text{(for shaft 1)},$$

$$[m_e]_2 = \begin{matrix} \ddot{\bar{\theta}}_2 & \ddot{\bar{\theta}}_3 \end{matrix} \begin{bmatrix} R_2^2 I_2' & 0 \\ 0 & I_3 \end{bmatrix} \begin{matrix} \ddot{\bar{\theta}}_2, \\ \ddot{\bar{\theta}}_3 \end{matrix} \quad [k_e]_2 = \begin{matrix} \bar{\theta}_2 & \bar{\theta}_3 \end{matrix} \begin{bmatrix} R_2^2 k_2 & R_2 k_2 \\ R_2 k_2 & k_2 \end{bmatrix} \begin{matrix} \bar{\theta}_2 \\ \bar{\theta}_3 \end{matrix} \quad \text{(for shaft 2)},$$

$$[m_e]_3 = \begin{matrix} \ddot{\bar\theta}_3 & \ddot{\bar\theta}_4 \end{matrix} \begin{bmatrix} 0 & 0 \\ 0 & I_4 \end{bmatrix} \begin{matrix} \ddot{\bar\theta}_3 \\ \ddot{\bar\theta}_4 \end{matrix} \quad [k_e]_3 = \begin{matrix} \bar\theta_3 & \bar\theta_4 \end{matrix} \begin{bmatrix} k_3 & -k_3 \\ -k_3 & k_3 \end{bmatrix} \begin{matrix} \bar\theta_3 \\ \bar\theta_4 \end{matrix} \quad \text{(for shaft 3)},$$

$$[m_e]_4 = \begin{matrix} \ddot{\bar\theta}_4 & \ddot{\bar\theta}_5 \end{matrix} \begin{bmatrix} 0 & 0 \\ 0 & I_5 \end{bmatrix} \begin{matrix} \ddot{\bar\theta}_4 \\ \ddot{\bar\theta}_5 \end{matrix} \quad [k_e]_4 = \begin{matrix} \bar\theta_4 & \bar\theta_5 \end{matrix} \begin{bmatrix} k_4 & -k_4 \\ -k_4 & k_4 \end{bmatrix} \begin{matrix} \bar\theta_4 \\ \bar\theta_5 \end{matrix} \quad \text{(for shaft 4)},$$

$$[m_e]_5 = \begin{matrix} \ddot{\bar\theta}_2 & \ddot{\bar\theta}_6 \end{matrix} \begin{bmatrix} R_5^2 I_2' & 0 \\ 0 & I_6 \end{bmatrix} \begin{matrix} \ddot{\bar\theta}_2, \\ \ddot{\bar\theta}_6 \end{matrix} \quad [k_e]_5 = \begin{matrix} \bar\theta_2 & \bar\theta_6 \end{matrix} \begin{bmatrix} R_5^2 k_5 & R_5 k_5 \\ R_5 k_5 & k_5 \end{bmatrix} \begin{matrix} \bar\theta_2 \\ \bar\theta_6 \end{matrix} \quad \text{(for shaft 5)},$$

$$[m_e]_6 = \begin{matrix} \ddot{\bar\theta}_6 & \ddot{\bar\theta}_7 \end{matrix} \begin{bmatrix} R_6^2 I_6' & 0 \\ 0 & I_7 \end{bmatrix} \begin{matrix} \ddot{\bar\theta}_6, \\ \ddot{\bar\theta}_7 \end{matrix} \quad [k_e]_6 = \begin{matrix} \bar\theta_6 & \bar\theta_7 \end{matrix} \begin{bmatrix} R_6^2 k_6 & R_6 k_6 \\ R_6 k_6 & k_6 \end{bmatrix} \begin{matrix} \bar\theta_6 \\ \bar\theta_7 \end{matrix} \quad \text{(for shaft 6)}. \tag{14}$$

To determine the overall property matrices of a structural system by using the FEM, one must input the coefficients of the elemental mass matrices $[m_e]_i$ and the elemental stiffness matrices $[k_e]_i$, $i = 1, 2, \ldots$, together with the identification numbers for the d.o.f. relating to these coefficients. The latter are denoted by the subscripts (j) of $\bar\theta_j$(j = 1–7) as shown on the upper side and right side of $[m_e]_i$ and $[k_e]_i$, i = 1–6, given by equation (14). From Figure 2(c), one sees that disk 3 is connected with shafts (2) and (3), while disk 4 is connected with shafts (3) and (4). Hence, if the mass moments of inertia for disks 3 and 4, I_3 and I_4, are incorporated with shafts (2) and (3), respectively, they should not be considered by shafts (3) and (4), respectively, again to avoid the repetition. This is the reason why the coefficients of first row and first column in the elemental mass matrices $[m_e]_3$ and $[m_e]_4$ are all equal to zero, as one may see from equation (14).

Assembling the mass matrices $[m_e]_i$ and stiffness matrices $[k_e]_i$, $i = 1, 2, \ldots$, for all the shaft elements as shown in equation (14) will determine the overall mass matrix $[\bar m]$ and overall stiffness matrix $[\bar k]$ and define the equation of motion of the entire vibration system:

$$[\bar m]\{\ddot{\bar\theta}\} + [\bar k]\{\bar\theta\} = 0. \tag{15}$$

For free vibration, one has

$$\{\bar\theta(t)\} = \{\bar\theta^*\} e^{i\omega t}, \tag{16}$$

where $\{\bar\theta^*\}$ is the amplitude of $\{\bar\theta(t)\}$, ω is the natural frequency of the system, t is time, and $i = \sqrt{-1}$.

Substitution of equation (16) into equation (15) leads to

$$([\bar k] - \omega^2[\bar m])\{\bar\theta^*\} = 0 \tag{17}$$

which is an eigenvalue equation, the solution ω_r represents the rth natural frequency and $\{\bar\theta^*\}_r$ the corresponding mode shape of the vibration system. Here the eigenvalue equation (17) is solved with the modified Jacobi method [17].

4. EIGENVALUES AND EIGENVECTORS OF THE DAMPED SYSTEM

The equation of motion for the free vibration of a damped system is given by

$$[\bar{m}]\{\ddot{\bar{\theta}}\} + [\bar{c}]\{\dot{\bar{\theta}}\} + [\bar{k}]\{\bar{\theta}\} = 0. \tag{18}$$

If the following equality equation is introduced

$$[\bar{m}]\{\dot{\bar{\theta}}\} - \{\bar{m}\}\{\dot{\bar{\theta}}\} = 0, \tag{19}$$

then the combination of equations (18) and (19) gives

$$[\tilde{m}]\{\dot{\Theta}\} + [\tilde{k}]\{\Theta\} = 0, \tag{20}$$

where

$$[\tilde{m}] = \begin{bmatrix} [0]_{n\times n} & [\bar{m}]_{n\times n} \\ [\bar{m}]_{n\times n} & [\bar{c}]_{n\times n} \end{bmatrix}_{2n\times 2n}, \quad [\tilde{k}] = \begin{bmatrix} -[\bar{m}]_{n\times n} & [0]_{n\times n} \\ [0]_{n\times n} & [\bar{k}]_{n\times n} \end{bmatrix}_{2n\times 2n}, \tag{21), (22}$$

$$\{\Theta\} = \begin{Bmatrix} \{\dot{\bar{\theta}}\} \\ \{\bar{\theta}\} \end{Bmatrix}_{2n\times 1}. \tag{23}$$

Subscript n in equations (21)–(23) represents the order of the matrix $[\bar{m}]$, $[\bar{c}]$ or $[\bar{k}]$. For free vibration, $\{\Theta(t)\}$ takes the form

$$\{\Theta(t)\} = \{\Theta^*\}e^{\alpha t}, \tag{24}$$

where $\{\Theta^*\}$ is the amplitude of $\{\Theta(t)\}$ and is a $2n \times 1$ column vector. The substitution of the last equation into equation (20) yields

$$([\tilde{k}] + \alpha_i[\tilde{m}])\{\Theta^*\}^{(i)} = 0 \tag{25}$$

which is an eigenequation with eigenvalues to take the following complex form:

$$\alpha_{\substack{2r \\ 2r-1}} = \bar{\omega}_{Rr} \pm i\bar{\omega}_{Ir} \quad (r = 1\text{–}n) \tag{26}$$

and the corresponding eigenvectors are

$$\{\Theta^*\}^{(2r)}_{(2r-1)} = \{\Theta^*\}^{(r)}_R \pm i\{\Theta^*\}^{(r)}_I = \begin{Bmatrix} \{\alpha\phi\} \\ \{\phi\} \end{Bmatrix}^{(r)}_R \pm i\begin{Bmatrix} \{\alpha\phi\} \\ \{\phi\} \end{Bmatrix}^{(r)}_I \quad (r = 1\text{–}n), \tag{27}$$

where $\bar{\omega}_{Ir}$ denote the $2r$th and $(2r-1)$th natural frequencies, while $\{\phi\}^{(r)}_I$ and $\{\alpha\phi\}^{(r)}_I$ denote the corresponding mode shapes of angular displacements and angular velocities [7].

5. FORCED VIBRATION RESPONSES

Based on the overall mass matrix $[\bar{m}]$, damping matrix $[\bar{c}]$ and stiffness matrix $[\bar{k}]$, one obtains the equation of motion for the forced vibration system

$$[\bar{m}]\{\ddot{\bar{\theta}}\} + [\bar{c}]\{\dot{\bar{\theta}}\} + [\bar{k}]\{\bar{\theta}\} = \{\bar{F}(t)\}, \tag{28}$$

where $\{\bar{F}(t)\}$ is the external load vector. Here, the Newmark direct integration method [17] is used to solve the dynamic responses.

6. THE EQUIVALENT DISK OF I AND THE EQUIVALENT SHAFT OF k

For the dynamic analysis of a torsional system, the key parameter of the disk is the polar mass moment of inertia, I, and that of the shaft is the torsional spring constant, k. Hence, most of the existing literature provides the values of I and k instead of the actual dimensions of each disk and each shaft. In order to study the influence on the dynamic behavior of the ratio between the polar mass moment of inertia of each shaft and that of the associated gear, each value of I is replaced by an "equivalent disk (or gear)" with diameter D and thickness T, while each value of k is also replaced by an "equivalent shaft" with diameter d and length l.

If the mass density of the disk (and the shaft) is ρ, then the polar mass moment of inertia of the jth disk is given by [2, 3]

$$I_j = \rho\left(\frac{\pi D_j^4}{32}\right)T_j. \tag{29}$$

From the last equation one obtains

$$D_j = \sqrt[4]{\left(\frac{32}{\rho\pi}\right)\left(\frac{I_j}{T_j}\right)}. \tag{30}$$

Similarly, the torsional spring constant of the ith shaft is [2, 3]

$$k_i = G\left(\frac{\pi d_i^4}{32}\right)\Big/ l_i. \tag{31}$$

Hence,

$$d_i = \sqrt[4]{\frac{32}{G\pi}k_i l_i}. \tag{32}$$

Where G is the shear modulus of the shaft material.

From equation (30) one sees that corresponding to one value of polar mass moment of inertia, I_j, a number of disks with different values of diameter D_j and thickness T_j may be obtained. Similarly, with respect to one value of torsional spring constant, k_i, one may have many shafts with different values of diameter d_i and length l_i as may be seen from equation (32). It is noted that the torsional spring constant of a shaft element is a key parameter that must always be considered for the torsional vibration analysis. However, the mass of the shaft element is often neglected in the most of the existing literature.

6.1. INFLUENCE OF SHAFT MASS ON THE NATURAL FREQUENCIES

For the shaft element (p) as shown in Figure 1(a) with damping effect neglected, the equation of free vibration is given by (cf. equation (1))

$$\begin{bmatrix} I_i + \frac{1}{3}I_p & \frac{1}{6}I_p \\ \frac{1}{6}I_p & I_j + \frac{1}{3}I_p \end{bmatrix}\begin{Bmatrix} \ddot{\theta}_i \\ \ddot{\theta}_j \end{Bmatrix} + \begin{bmatrix} k_p & -k_p \\ -k_p & k_p \end{bmatrix}\begin{Bmatrix} \theta_i \\ \theta_j \end{Bmatrix} = 0. \tag{33}$$

For harmonic free vibration, one has

$$\begin{Bmatrix}\theta_i(t)\\ \theta_j(t)\end{Bmatrix} = \begin{Bmatrix}\theta_i^*\\ \theta_j^*\end{Bmatrix} e^{i\omega t}, \tag{34}$$

where θ_i^* and θ_j^* are, respectively, the amplitudes of $\theta_i(t)$ and $\theta_j(t)$, ω is the natural frequency of the shaft element, t is time, and $i = \sqrt{-1}$.

Substituting equation (34) into equation (33) gives

$$\begin{bmatrix} k_p - \omega^2(I_i + \frac{1}{3}I_p) & -k_p - \omega^2(\frac{1}{6}I_p) \\ -k_p - \omega^2(\frac{1}{6}I_p) & k_p - \omega^2(I_j + \frac{1}{3}I_p)\end{bmatrix}\begin{Bmatrix}\theta_i^*\\ \theta_j^*\end{Bmatrix} = 0. \tag{35}$$

Non-trivial solution of the last equation requires that

$$\begin{vmatrix} k_p - \omega^2(I_i + \frac{1}{3}I_p) & -k_p - \omega^2(\frac{1}{6}I_p) \\ -k_p - \omega^2(\frac{1}{6}I_p) & k_p - \omega^2(I_j + \frac{1}{3}I_p)\end{vmatrix} = 0. \tag{36}$$

From the last equation one obtains

$$\omega = 0 \tag{37}$$

and

$$\omega_C = \sqrt{\frac{k_p(I_i + I_j + I_p)}{I_i I_j + \frac{1}{3}(I_i + I_j)I_p + \frac{1}{12}I_p^2}}, \tag{38}$$

where $\omega = 0$ represents the natural frequency of the rigid-body motion, while ω_C denotes the natural frequency of "considering" the shaft mass. For the case of "neglecting" the shaft mass, i.e., $I_p = 0$, equation (38) reduces to

$$\omega_N = \sqrt{\frac{k_p(I_i + I_j)}{I_i I_j}} \tag{39}$$

which is the natural frequency of a torsional system composed of two rigid disks (with mass moments of inertia, I_i and I_j) connected by a "massless' shaft (with spring constant k_p) as one may see from the textbook [3].

From equations (38) and (39) one obtains the ratio of ω_N (by "neglecting" the shaft mass) to ω_C (by "considering" the shaft mass) to be

$$R_\omega = \frac{\omega_N}{\omega_C} = \sqrt{\left(\frac{\bar{I}_i + \bar{I}_j}{\bar{I}_i + \bar{I}_j + 1}\right)\left(\frac{\bar{I}_i\bar{I}_j + \frac{1}{3}(\bar{I}_i + \bar{I}_j) + \frac{1}{12}}{\bar{I}_i\bar{I}_j}\right)}, \tag{40}$$

where

$$\bar{I}_i = I_i/I_p, \quad \bar{I}_j = I_j/I_p. \tag{41}$$

Although both the natural frequencies ω_N and ω_C are functions of torsional spring constant k_p (see equations (38) and (39)), however, the ratio between them, $R_\omega (= \omega_N/\omega_C)$, has nothing to do with k_p as one may see from equation (40).

For convenience, the two dimensionless parameters $\bar{I}_i$ and $\bar{I}_j$ defined by equation (41) are replaced by

$$R_{p/i} = 1/\bar{I}_i = I_p/I_i \tag{42}$$

and

$$R_{j/i} = \bar{I}_j/\bar{I}_i = I_j/I_i, \tag{43}$$

where $R_{p/i}$ and $R_{j/i}$ represent the ratios of the mass moments of inertia of shaft p and the larger gear (or disk) j to the one of the smaller gear (or disk) i respectively. Use of equations (42) and (43) reduces equation (40) to

$$R_\omega = \frac{\omega_N}{\omega_C} = \sqrt{\left(\frac{1 + R_{j/i}}{1 + R_{j/i} + R_{p/i}}\right)\left(\frac{R_{j/i} + \frac{1}{3}(1 + R_{j/i})R_{p/i} + \frac{1}{12}R_{p/i}^2}{R_{j/i}}\right)}. \tag{44}$$

Hence, for a two-d.o.f. (2-d.o.f.) shaft system with all its dimensions keeping unchanged except the shaft diameter, one may determine the influence of the shaft mass on the natural frequency from the last equation.

7. NUMERICAL RESULTS AND DISCUSSIONS

A three-branched gear system as shown in Figure 2(a) [2] and a six-branched one as shown in Figure 3 [13] are studied in this paper. The material constants for the gears and the shaft segments are: mass density $\rho = 0{\cdot}73 \times 10^{-3}$ lbs^2/in^4, shear modulus of elasticity $G = 1{\cdot}15 \times 10^7$ psi. The other given data are listed in Tables 1 and 5 respectively.

7.1. FREE VIBRATION ANALYSIS OF AN UNDAMPED THREE-BRANCHED SYSTEM

For the three-branched gear system shown in Figure 2(a), the principal dimensions and the physical properties of the gears and the shafts are listed in Table 1. Actually, the only data given by Wilson [2] are the mass moments of inertia for the gears, I_j (j = 1–10), and the spring constants, k_i (i = 1–6), as shown in the second and sixth Columns of Table 1. The other data (such as gear thickness T_j, gear diameter D_j, shaft diameter d_i and shaft length l_i as shown in third, fourth, seventh and eighth columns of Table 1) are calculated by using equations (30) and (32) for studying the influence of the shaft mass on the natural frequencies of the system.

Based on the present approach, the gear-branched system shown in Figure 2(a) is reduced to the equivalent direct-transmitted gear system shown in Figure 2(c). It is seen that the three slave gears (Nos. 3, 7 and 9 of Figure 2(a)) are eliminated in the equivalent system (Figure 2(c)). The natural frequency of rigid-body motion, ω_0, and those of the lowest five elastic torsional vibrations, ω_r (r = 1–5), are listed in Table 2. For the case of "neglecting" the shaft mass, it is seen that the natural frequencies $\omega_{r,N}$ (r = 1–5) obtained from the present approach are in good agreement with those obtained from the FEM of reference [16] or from the Holzer method of reference [2]. For the case of "considering" the shaft mass, the natural frequencies $\omega_{r,C}$ (r = 1–5) obtained from the present approach are shown in the third row of Table 2. The digits placed in the parentheses ( ) represent the ratios of $\omega_{r,N}$ to $\omega_{r,C}$. Since all the values of $R_{\omega r} = \omega_{r,N}/\omega_{r,C}$ (r = 1–5) are greater than 1·0, the shaft mass has the effect of reducing the natural frequencies of the torsional system. However, since $R_{\omega r} = \omega_{r,N}/\omega_{r,C} \approx 1.0$, the influence of shaft mass on the dynamic behavior of the present torsional system is negligible.

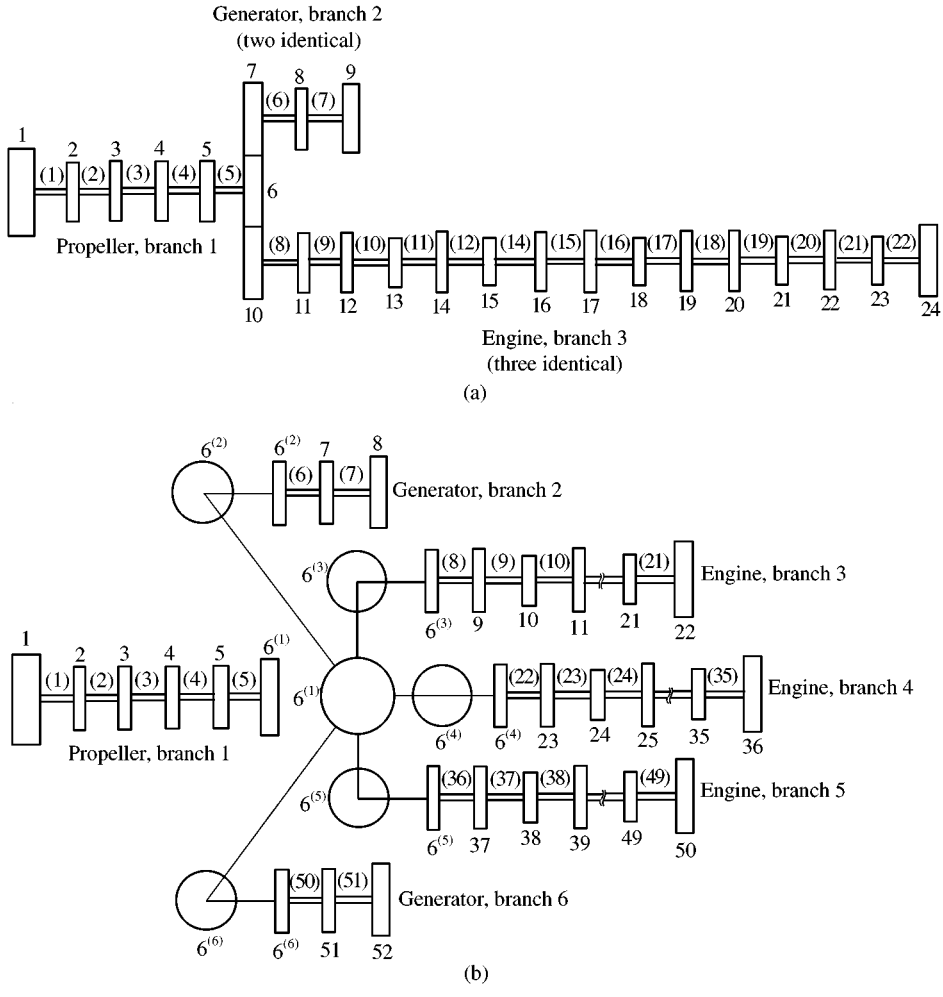

Figure 3. (a) The mathematical model of a six-branched gear system; and (b) the equivalent direct-transmitted gear system (i.e., the FEM model).

The rigid-body mode shape $\{\bar{\theta}^*\}_0$ and the lowest four elastic mode shapes $\{\bar{\theta}^*\}_r$ ($r = 1$–4) are shown in Table 3 and Figure 4. From Figure 4(c) one sees that the second mode displacements at disks, 1, 4 and 5 are predominant. This may be the main reason that the dampers equipped on these three disks as shown in Figure 5 affects the second natural frequency ω_2 significantly as may be seen from Table 4.

7.2. FREE VIBRATION ANALYSIS OF AN UNDAMPED SIX-BRANCHED SYSTEM

The next example illustrated here is the six-branched gear system as shown in Figure 3(a) with the dimensions and physical properties listed in Table 5. The corresponding equivalent direct-transmitted gear system is shown in Figure 3(b). It is similar to Table 1 in that the given data are the mass moments of inertia of the gears, I_j ($j = 1$–24), and the spring constants of the shaft segments, k_i ($i = 1$–21), as shown in the second and sixth columns of

TABLE 1

The dimensions and physical properties for the three-branched gear system as shown in Figure 2(a)

Gears				Shafts			
No.† j	Mass moments of inertia, I_j (lb in s^2)	Thickness T_j (in)	Diameters‡ D_j (in)	No. i	Spring constants, k_i 10^6 (lb in/rad)	Diameters d_i (in)	Lengths l_i (in)
1	9720·0	7	66·345	1	5·46	5	129·236
2	986·4	2	51·218	2	1·74	4	166·107
3	36·0	2·108	22·094	3	35·28	4	8·192
4	402·0	2	40·923	4	68·70	4	4·207
5	234·0	2	35·745	5	1·94	4	148·983
6	234·0	2	35·745	6	2·15	2·5	20·513
7	3·6	3·934	10·6301				
8	300·0	0·78856	48·000				
9	0·36	4·9178	5·6533				
10	81·6	2	27·468				

†The disk numbering is based on the original gear-branched system (including the slave gears) as shown in Figure 2(a).

‡Gear ratios: $R_2 = D_2/D_3 = 2{\cdot}3182$, $R_5 = D_2/D_7 = 4{\cdot}8182$, $R_6 = D_8/D_9 = 8{\cdot}4906$.

TABLE 2

Several lowest natural frequencies of the three-branched gear system as shown in Figure 2(a), ω_r ($r = 0$–5)

Methods	Natural frequencies ω_r (rad/s)						Shaft mass
	ω_0	ω_1	ω_2	ω_3	ω_4	ω_5	
Present	0·000	23·0870	41·2902	215·2224	376·6524	710·4786	Considered†
	0.000	23·0899	41·3228	217·6013	376·9155	712·6985	Neglected‡
		(1·000)§	(1·001)	(1·011)	(1·001)	(1·003)	
FEM [16]	0·000	23·0899	41·3228	217·6013	376·9155	712·6985	Neglected‡
		(1·000)§	(1·001)	(1·011)	(1·001)	(1·003)	
Holzer [2]	0·000	23·0929	41·3290	217·9722	376·9155	713·3585	Neglected‡
		(1·000)§	(1·001)	(1·013)	(1·001)	(1·004)	

†Mass of each shaft segment is "considered".

‡Mass of each shaft segment is "neglected".

§Ratios evaluated from the formula: $R_{\omega r} = \omega_{r,N}/\omega_{r,C}$, $r = 1$–5, where subscripts C and N denote that the mass of each shaft segment is "considered" and "neglected" respectively.

Table 5. The other dimensions of the gears and shafts are calculated by using equations (30) and (32).

For the equivalent gear system shown in Figure 3(b), the reduction gear of branch 1 (designated by $6^{(1)}$) meshes with the others of branches 2–6, $6^{(j)}$ ($j = 2$–6), with gear ratios $R_j = D_6^{(1)}/D_6^{(j)} = 5{\cdot}0$ ($j = 2$–6). If the reduction gear $6^{(1)}$ is considered as the master gear, then the others $6^{(j)}$ ($j = 2$–6) are the slave gears and should be eliminated from the

TABLE 3

Several lowest mode shapes for the three-branched gear system as shown in Figure 2(a), $\{\bar{\theta}^*\}_r$ $(r = 0\text{–}4)$

Disk no†. j	$\{\bar{\theta}^*\}_0$	$\{\bar{\theta}^*\}_1$	$\{\bar{\theta}^*\}_2$	$\{\bar{\theta}^*\}_3$	$\{\bar{\theta}^*\}_4$
1	0·10000E + 01	0·10000E + 01	0·10000E + 01	0·10000E + 01	0·10000E + 01
2	0·10000E + 01	0·50885E − 01	− 0·20399E + 01	− 0·83294E + 02	− 0·25191E + 03
3	− 0·23182E + 01	− 0·11796E + 00	0·47288E + 01	0·19309E + 03	0·58397E + 03
4	− 0·23182E + 01	− 0·16109E + 00	0·35250E + 02	− 0·35264E + 01	− 0·75079E + 04
5	− 0·23182E + 01	− 0·16224E + 00	0·36069E + 02	− 0·11321E + 02	0·42466E + 04
6	− 0·23182E + 01	− 0·16254E + 00	0·36280E + 02	− 0·13498E + 02	0·82280E + 04
7	− 0·48182E + 01	− 0·24518E + 00	0·98284E + 01	0·40133E + 03	0·12137E + 04
8	− 0·48182E + 01	0·33151E + 00	− 0·20376E + 01	0·23176E + 01	0·16137E + 02
9	0·40909E + 02	− 0·28147E + 01	0·17301E + 02	− 0·19677E + 02	− 0·13701E + 03
10	0·40909E + 02	− 0·28728E + 01	0·18499E + 02	0·24686E + 02	0·31196E + 02

†The numbering is based on the original gear-branched system (including the slave gears) as shown in Figure 2(a).

equivalent system based on the present approach. For this reason, the total number of "independent" gears shown in Figure 3(b) is 52 (=57–5).

The natural frequency of rigid-body motion, ω_0, and those of the lowest five elastic torsional vibrations, ω_r $(r = 1\text{–}5)$, are listed in Table 6, while the associated mode shapes, $\{\bar{\theta}^*\}_r$ $(r = 0\text{–}4)$, are shown in Figure 6. For the case of "neglecting" the shaft mass, the lowest five elastic natural frequencies $\omega_{r,N}$ $(r = 1\text{–}5)$ obtained from the present approach (see the fourth row of Table 6) are in good agreement with those obtained from the FEM of reference [16] (see the sixth row of Table 6). However, the CPU time required by the former (9 s) is much less than that required by the latter (35 s) as one may see from the final column of Table 6. The computer used here is the Pentium 133 with 16 MB RAM. In other words, the calculating speed used in the present approach is about four times higher than that used in the method of reference [16]. This is because neither element-by-element transformations nor overall transformation is required for the present approach.

For the case of "considering" the shaft mass, the lowest five natural frequencies $\omega_{r,C}$ $(r = 1\text{–}5)$ obtained from the present approach are shown in the third row of Table 6. From the ratios $R_{\omega r} = \omega_{r,N}/\omega_{r,C}$ $(r = 1\text{–}5)$ shown in the parentheses $(\cdot)$ of Table 6 for the six-branched gear system, one sees that the present values of $R_{\omega r}$ $(r = 1\text{–}5)$ are much larger than the corresponding values shown in Table 2 for the three-branched system. This result agrees with that shown in Tables 7 and 8.

Comparing Figure 6 with Figure 3(a), one sees that disk Nos. 1–6 belong to the propeller branch (i.e., branch No. 1), while disk Nos. 7–9 and 55–57 (see Figure 6), respectively, belong to the generator branches (i.e., branch Nos. 2 and 6) as shown in Figure 3(b). The disk numbers of the other three engine branches (see Figure 3(b)) are 10–24 (for branch No. 3), 25–39 (for branch No. 4), 40–54 (for branch No. 5), respectively, as shown in Figure 6. Figure 6(a) shows the rigid-body mode (or 0th mode). It is evident that the directions of the angular displacements of disk Nos. 7, 10, 25, 40 and 55 (that is, the directions of $\bar{\theta}_j^*, j = 7, 10, 25, 40, 55$) are the same and are opposite to the direction of the angular displacement of disk No. 6 (that is the direction of $\bar{\theta}_6^*$). Also, the amplitudes of the former are the same and are much larger than the amplitude of the latter. This is because disk Nos. 7, 10, 25, 40 and 55

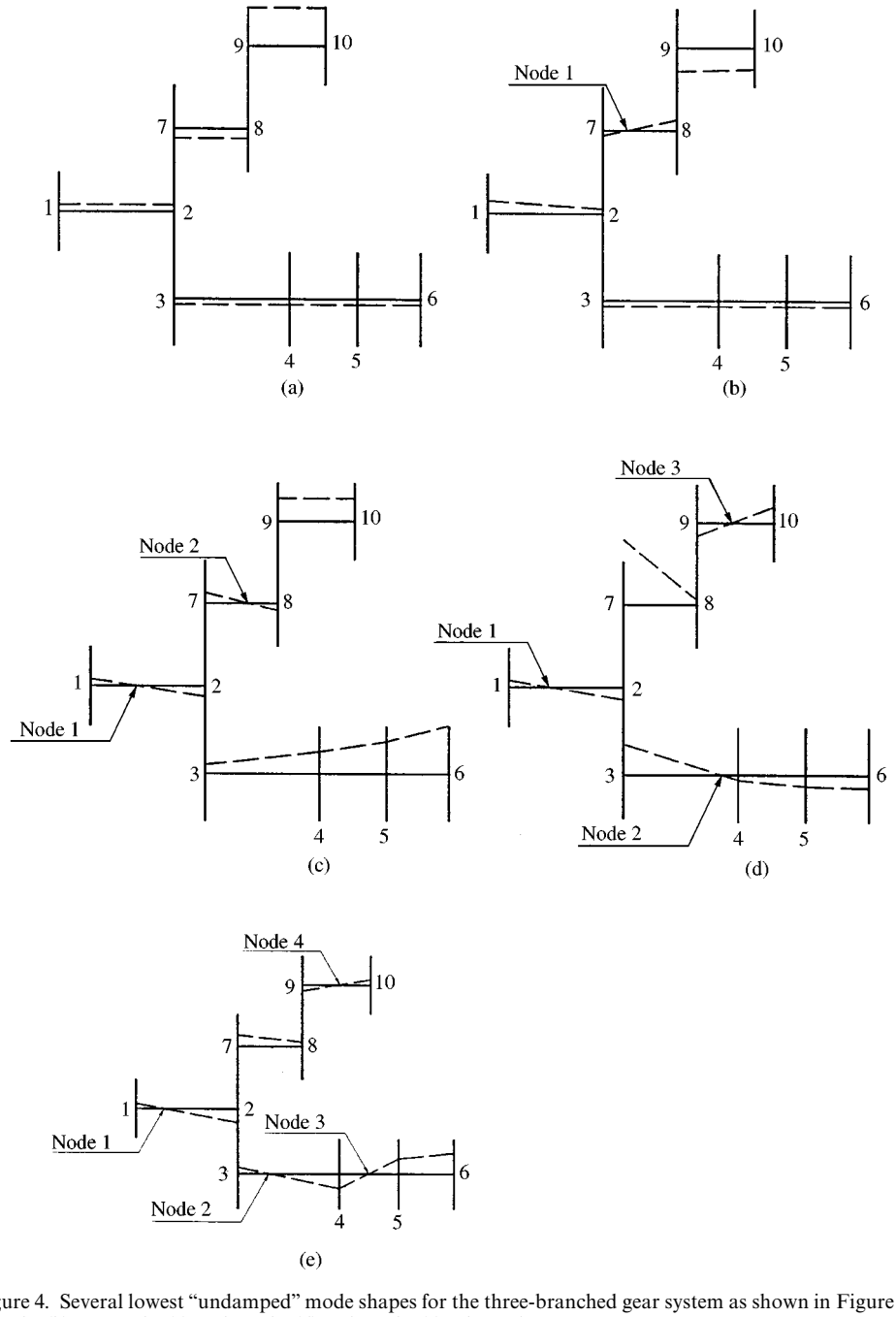

Figure 4. Several lowest "undamped" mode shapes for the three-branched gear system as shown in Figure 2: (a) 0th mode; (b) 1st mode; (c) 2nd mode; (d) 3rd mode; (e) 4th mode.

are meshed with disk No. 6 and the diameters of the former are the same ($D_j = 16{\cdot}1405''$) and are much smaller than the diameter of disk No. 6 ($D_6 = 80{\cdot}7026''$) as one may see from Table 5. The foregoing phenomena exist in mode shapes 1–4 shown in Figure 6(b)–6(e), since they are the compatibility conditions that each mode shape must satisfy.

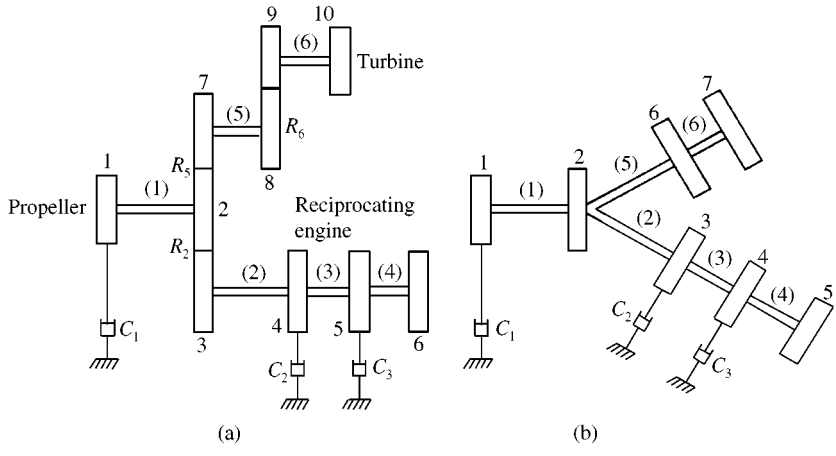

Figure 5. (a) The mathematical model of a damped three-branched gear system; and (b) the equivalent direct-transmitted gear system (or the FEM model).

TABLE 4

Influence of damping on the natural frequencies of the three-branched gear system as shown in Figure 5(a) with the shaft mass considered

Damping coeff. C_j ($j = 1$–3) (lb in s/rad)	Eigenvalues $\alpha_r = \bar{\omega}_{Rr} \pm i\bar{\omega}_{Ir}$					Remarks
	α_1	α_2	α_3	α_4	α_5	
8000	− 0·3998 23·0966 (1·0004)†	− 8·7961 40·5066 (0·9810)	− 0·0619 215·1637 (0·9997)	− 6·9392 376·5910 (0·9998)	− 0·0412 710·4205 (0·9999)	ω_{Rr} ω_{Ir} (rad/s)
12 000	− 0·5976 23·0985 (1·0005)	− 13·2015 39·1429 (0·9480)	− 0·0978 215·2030 (0·9999)	− 10·3994 376·5661 (0·9998)	− 0·00596 710·4504 (0·9999)	ω_{Rr} ω_{Ir} (rad/s)
16 000	− 0·7951 23·0915 (1·0002)	− 17·6025 37·1352 (0·8994)	− 0·1284 215·2301 (1·0000)	− 13·8619 376·4578 (0·9995)	− 0·02012 710·3591 (0·9998)	ω_{Rr} ω_{Ir} (rad/s)
20 000	− 0·9913 23·0878 (1·0000)	− 22·0224 34·3940 (0·8330)	− 0·1564 215·2120 (0·9999)	− 17·3323 376·3601 (0·9992)	− 0·0455 710·4620 (0·9999)	ω_{Rr} ω_{Ir} (rad/s)
24 000	− 1·1874 23·0811 (0·9997)	− 26·4465 30·6837 (0·7431)	− 0·1860 215·1843 (0·9998)	− 20·7890 376·2430 (0·9989)	− 0·0299 710·4676 (0·9999)	ω_{Rr} ω_{Ir} (rad/s)
28 000	− 1·3816 23·0706 (0·9993)	− 30·8628 25·5747 (0·6194)	− 0·2144 215·1736 (0·9998)	− 24·2511 376·1337 (0·9986)	− 0·0163 710·3758 (0·9998)	ω_{Rr} ω_{Ir} (rad/s)
Undamped natural frequency	23·0870	41·2902	215·2224	376·6524	710·4786	ω_{0r} (rad/s)

†Digits in the parentheses ( ) are the ratios of ω_{Ir}/ω_{0r} ($r = 1$–5), where ω_{0r} are the undamped natural frequencies listed in Table 2 and the final row of the present table.

TABLE 5

The dimensions and physical properties for the six-branched gear system as shown in Figure 3(a)

Branches No.‡ j	Gears: Mass moments of inertia, I_j (lb in s^2)	Gears: Thickness T_j (in)	Gears: Diameter† D_j (in)	Shafts: No. i	Shafts: Spring constant, k_i 10^7 (lb in/rad)	Shafts: Diameter d_i (in)	Shafts: Length l_i (in)
Propeller branch							
1	48000·00	20·0	76·072	1	20·964	9·701	47·70
2	4000·00	5·0	57·802	2	47·393	9·701	21·10
3	1478·00	5·0	45·066	3	10·917	9·701	91·60
4	672·00	2·0	46·532	4	7·570	9·701	132·10
5	374·00	2·0	40·191	5	60·976	9·701	16·40
6	3040·00	1·0	80·7026				
Generator branch							
7	300·00	61·6780	16·1405	6	36·765	9·701	27·20
8	38·56	2·0	22·774	7	1·575	9·701	635·0
9	1408·00	5·0	44·522				
Engine branch							
10	300·00	61·6780	16·1405	8	58·140	9·701	17·20
11	272·80	2·0	37·143	9	175·439	9·701	5·70
12	16·40	2·0	18·392	10	1·600	9·701	625·00
13	108·40	2·0	29·490	11	107·527	9·701	9·30
14	1483·60	2·0	56·721	12	185·185	9·701	5·40
15	80·32	2·0	27·360	13	142·857	9·701	7·00
16	80·32	2·0	27·360	14	142·857	9·701	7·00
17	80·32	2·0	27·360	15	142·857	9·701	7·00
18	80·32	2·0	27·360	16	142·857	9·701	7·00
19	80·32	2·0	27·360	17	142·857	9·701	7·00
20	80·32	2·0	27·360	18	142·857	9·701	7·00
21	80·32	2·0	27·360	19	142·857	9·701	7·00
22	80·32	2·0	27·360	20	105·263	9·701	9·50
23	9·80	2·0	16·170	21	2·959	9·701	338·00
24	183·60	2·0	33·642				

†Gear ratios: $R_j = D_6^{(1)}/D_6^{(j)} = 5{\cdot}0$ ($j = 2$–6) (see Figure 3(b)).
‡The numbering is based on the original gear-branched system (including the slave gears).

7.3. FREE VIBRATION ANALYSIS OF A DAMPED THREE-BRANCHED SYSTEM

To show the utility of the present approach for the damped system, the three-branched gear system as shown in Figure 2(a) equipped with three dampers is studied. Figure 5(a) shows the mathematical model of the original gear system and Figure 5(b) shows the equivalent direct-transmitted one. For convenience, the damping coefficients of the three dampers, C_j ($j = 1$–3), are assumed to be the same. The influence of damping on the lowest five (elastic) natural frequencies with shaft mass considered, ω_{Ir} ($r = 1$–5), of the three-branched gear system (see Figure 5) is shown in Table 4 for the cases of C_j ($j = 1$–3) = 8000–28 000 lb in s/rad. The real parts (ω_{Rr}) of the eigenvalues (α_r, $r = 1$–5) denote the rth damping parameter, and the imaginary parts (ω_{Ir}) denote the corresponding rth "damped" natural frequencies. For the convenience of comparison, the lowest five "undamped" natural frequencies (with shaft mass considered), ω_{0r} ($r = 1$–5), obtained from Table 2 are also listed in the final row of Table 4.

TABLE 6

Several lowest natural frequencies for the six-branched gear system as shown in Figure 3 and the CPU time required

Methods	Natural frequencies ω_r (rad/s)						Shaft mass	CPU time (t)
	ω_0	ω_1	ω_2	ω_3	ω_4	ω_5		
Present	0·000	26·4662	72·9823	72·9852	88·0565	98·7648	Considered†	9 s
	0·000	26·8301	78·8936	78·8960	93·6692	103·5667	Neglected‡	9 s
		(1.014)§	(1·081)	(1·081)	(1·064)	(1·049)		
FEM [16]	0·000	26.8301	78·8965	78·8965	93·6667	103.5604	Neglected‡	35 s
		(1·014)§	(1·081)	(1·081)	(1·064)	(1·049)		

†Mass of each shaft segment is "considered".
‡Mass of each shaft segment is "neglected".
§Ratios evaluated fro the formula $R_{\omega r} = \omega_{r,N}/\omega_{r,C}$ ($r = 1$–5), where subscripts C and N denote that the mass of each shaft segment is "considered" and "neglected" respectively.

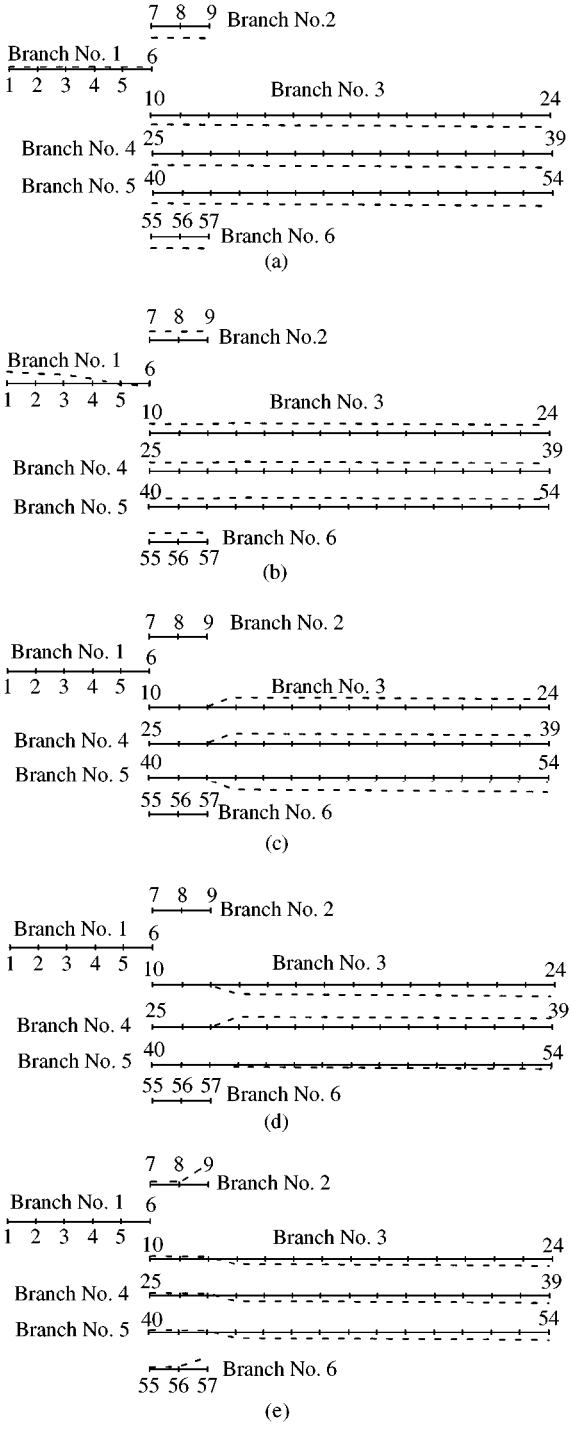

Figure 6. Several lowest mode shapes for the six-branched gear system as shown in Figure 3: (a) 0th mode $\{\bar{\theta}^*\}_0$; (b) 1st mode $\{\bar{\theta}^*\}_1$; (c) 2nd mode $\{\bar{\theta}^*\}_2$; (d) 3rd mode $\{\bar{\theta}^*\}_3$; and (e) 4th mode $\{\bar{\theta}^*\}_4$.

TABLE 7

Influence of shaft mass on the lowest five natural frequencies for the three-branched gear system as shown in Figure 2(a) with $d_6 = 4'' = constant$

Shaft dia. d_i $(i = 1–5)$	Natural frequencies ω_r (rad/s) ω_1	ω_2	ω_3	ω_4	ω_5	Shaft mass
	15·2918	41·0561	210·3093	376·6550	828·2767	Considered
4″	15·2945	41·0961	212·5264	376·9178	828·3726	Neglected
	(1·000)†	(1·001)	(1·011)	(1·001)	(1·000)	
	23·8905	64·0633	323·4693	587·9341	1293·9670	Considered
5″	23·8963	64·1923	331·7351	588·9336	1294·3320	Neglected
	(1·000)	(1·002)	(1·026)	(1·002)	(1·000)	
	34·3949	92·0237	453·0417	845·0939	1788·8200	Considered
6″	34·4071	92·4027	476·7684	848·0631	1821·8510	Neglected
	(1·000)	(1·004)	(1·052)	(1·004)	(1·019)	
	46·7985	124·7472	590·4014	1146·8770	1788·5120	Considered
7″	46·8238	125·6931	646·6537	1154·3040	1829·7270	Neglected
	(1·001)	(1·008)	(1·095)	(1·007)	(1·023)	

†Ratios evaluated from the formula $R_{\omega r} = \omega_{r,N}/\omega_{r,C}$, $r = 1–5$.

TABLE 8

Influence of shaft mass on the lowest five natural frequencies for the six-branched gear system as shown in Figure 3(a)

Shaft dia. d_i $(i = 1 - 51)$	Natural frequencies ω_r (rad/s) ω_1	ω_2	ω_3	ω_4	ω_5	Shaft mass
	10·2392	29·8149	29·8153	35·4914	39·3284	Considered
6″	10·2632	30·1791	30·1795	35·8292	39·6137	Neglected
	(1·002)†	(1·012)	(1·012)	(1·010)	(1·007)	
	13·9109	40·1735	40·1747	47·9256	53·2056	Considered
7″	13·9699	41·0795	41·0000	48·7681	53·9187	Neglected
	(1·004)	(1·023)	(1·021)	(1·016)	(1·013)	
	18·1191	51·6772	51·6791	61·8497	68·8571	Considered
8″	18·2454	53·6509	53·6514	63·6960	70·4244	Neglected
	(1·007)	(1·038)	(1·038)	(1·030)	(1·023)	
	22·8492	64·0269	64·0295	76·9601	86·0147	Considered
9″	23·0923	67·9034	67·9045	80·6157	89·1308	Neglected
	(1·011)	(1·061)	(1·061)	(1·048)	(1·036)	

†Ratios evaluated from the formula $R_{\omega r} = \omega_{r,N}/\omega_{r,C}$, $r = 1–5$.

The ratios of "damped" natural frequencies ω_{Ir} to the corresponding "undamped" ones ω_{0r} are shown in the parentheses ( ) of Table 4. It is evident that most of the values of ω_{1r}/ω_{0r} $(r = 1–5)$ are less than 1·0 with very few exceptions. This is a reasonable result since the damping has the effect of reducing the natural frequencies of a vibration system. From Table 4 one also sees that the influence of damping on the second natural frequency ω_{I2} is much more predominant than that on the others (ω_{Ir}, $r = 1, 3, 4, 5$). This phenomenon may

have something to do with the relative positions of the three dampers [see Figure 5(a)] and the second mode shape of the three-branched gear system (see Figure 4(c)).

7.4. INFLUENCE OF SHAFT MASS ON THE NATURAL FREQUENCIES

For a torsional system composed of two rigid disks (with mass moments of inertia I_i and I_j, $I_i < I_j$) and a shaft segment (with spring constant k_p), the influence of the shaft mass (or shaft mass moment of inertia, I_p) on the natural frequencies of the system is shown in Figure 7, which is obtained on the basis of equation (44). The ordinate of the figure denotes the ratio of the natural frequency of the system with shaft mass "neglected", ω_N, to that with shaft mass "considered", ω_C, i.e., $R_\omega = \omega_N/\omega_C$; while the abscissa denotes the ratio of mass moment of inertia of the shaft segment, I_p, to that of the smaller disk, I_i, i.e., $R_{p/i} = I_p/I_i$. Each curve in Figure 7 denotes the relationship between R_ω and $R_{p/i}$ for a specified value of $R_{j/i} = I_j/I_i$, which is the ratio of the mass moment inertia of the larger disk, I_j, to that of the smaller disk, I_i. From Figure 7 one sees that the value of R_ω is related to both $R_{p/i}$ and $R_{j/i}$. However, the influence of $R_{p/i}$ on R_ω is much greater than that of $R_{j/i}$ on R_ω. For example, for the solid curve (with $R_{j/i} = 1{\cdot}0$), Figure 7 shows that $R_\omega = 1{\cdot}0075$ if $R_{p/i} = 0{\cdot}1$ and $R_\omega = 1{\cdot}08$ if $R_{p/i} = 1{\cdot}0$; but even if for the case of $R_{p/i} = 1{\cdot}0$ (i.e., $I_p = I_i$), Figure 7 shows that $R_\omega = 1{\cdot}08$ if $R_{j/i} = 1{\cdot}0$ and $R_\omega = 1{\cdot}12$ if $R_{j/i} = 9{\cdot}0$. In other words, the ratio of mass moment of inertia of the shaft segment, I_p, to that of the disk, I_i or I_j, will be the key parameter determining the influence of the shaft mass on the dynamic behavior of a torsional system.

Although the last statement is based on a 2-d.o.f. torsional system, it is also available for the m.d.o.f. systems as shown in Figures 2(a) and 3(a). For example, if all the physical quantities relating to the gears (or disks) and the length of each shaft segment as shown in

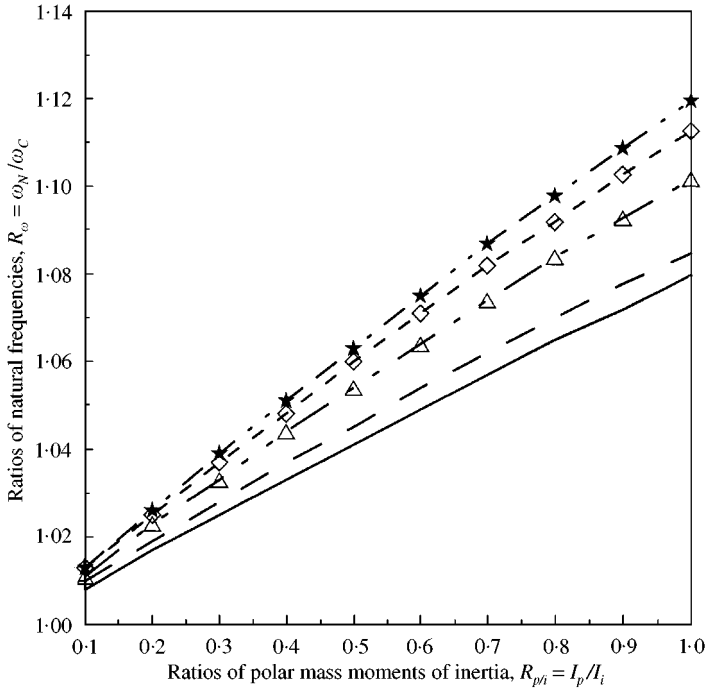

Figure 7. The influence of parameters $R_{p/i}$ and $R_{j/i}$ on the frequency ratio $R_\omega = \omega_N/\omega_C$: ——, $R_{j/i} = I_j/I_i = 1{\cdot}0$; —–, $R_{j/i} = I_j/I_i = 3{\cdot}0$; —△-, $R_{j/i} = I_j/I_i = 5{\cdot}0$; –◇–, $R_{j/i} = I_j/I_i = 7{\cdot}0$; –★–, $R_{j/i} = I_j/I_i = 9{\cdot}0$.

Table 1 are kept unchanged, while the diameters of all the shaft segments are simultaneously changed to 4″, 5″, 6″ and 7″, respectively, except that $d_6 = 4'' = \text{constant}$, and the torsional spring constant of each shaft element are recalculated by using equation (31), then the influence of the shaft mass (or I_p) on the natural frequencies of the three-branched gear system is as shown in Table 7. Because most of the values of $R_{\omega r} = \omega_{r,N}/\omega_{r,C}$ $(r = 1\text{–}5)$ are near 1·0, i.e., $\omega_{r,N} \approx \omega_{r,C}$ $(r = 1\text{–}5)$, the influence of the shaft mass on the natural frequencies of the three-branched system is negligible. However, the last trend is not true for the six-branched gear system shown in Figure 3(a), since most of the values of $R_{\omega r} = \omega_{r,N}/\omega_{r,C}$ $(r = 1\text{–}5)$ are greater than 1·0, i.e., $\omega_{r,N} > \omega_{r,C}$ $(r = 1\text{–}5)$, as one may see from the digits listed in the parentheses ( ) of Table 8. The last table is obtained with all the physical quantities relating to the gears (or disks) and the length of each shaft segment as shown in Table 5 are kept unchanged, while the diameters of all the shaft segments are simultaneously changed to 6″, 7″, 8″ and 9″, respectively, and the torsional spring constant of each shaft element is recalculated by using equation (31).

The foregoing phenomenon for the three- and six-branched gear systems may be explained with the help of Tables 9 and 10. For each shaft element, Table 9 lists the ratio of mass moment of inertia of the larger gear to that of the smaller gear, $R_{j/i} = I_j/I_i$, and the ratio of mass moment of inertia of the shaft segment to that of the smaller gear, $R_{p/i} = I_p/I_i$, for the three-branched system, while Table 10 gives the similar ratios for the six-branched system. Tables 9 and 10 are obtained on the assumption that the mass moment of inertia of any gear connecting with two adjacent shaft segments is equally divided into two parts and then each part connects with one shaft segment.

A comparison between Tables 9 and 10 shows that the values of $R_{p/i} = I_p/I_i$ for the three-branched gear system are much smaller than the corresponding ones for the six-branched system, hence the influence of shaft mass on three-branched system is much smaller than that on the six-branched system. It is noted that the last result is obtained based on the fact that the mass moments of inertia of the gears and the shaft segment of the sixth shaft element is much smaller than those of the other shaft elements for the three-branched system (see Figure 2(a) and Table 1), so that the effect of the unusual large value of $R_{j/i} = I_j/I_i = 226{\cdot}667$ for the sixth shaft element (see Table 9) is neglected.

7.5. FORCED VIBRATION ANALYSIS OF A DAMPED SYSTEM

For the three-branched damped gear system as shown in Figure 5, if an exciting torque $F(t) = 6000\ \sin(\omega_e t)$ lb-in is applied to disk 1, then the relationship between the maximum

TABLE 9

Ratios of mass moments of inertia between gears and shaft for each shaft element as shown in Figure 2(a) and Table 1

Numbering of shaft element	1	2	3	4	5	6
†$R_{j/i} = I_j/I_i$	9·854	5·583	1·718	2·0	83·333	226·667
‡$R_{p/i} = I_p/I_i$	0·00586	0·08466	0·00128	0·000658	0·7592	0·1583

†$R_{j/i} = I_j/I_i$ = ratio of mass moment of inertia of larger gear to that of smaller gear for each shaft element.
‡$R_{p/i} = I_p/I_i$ = ratio of mass moment of inertia of shaft to that of smaller gear for each shaft element.

TABLE 10

Ratios of mass moments of inertia between gears and shaft for each shaft element as shown in Figure 3(a) and Table 5

Numbering of shaft element	1	2	3	4	5	6	7	8
								22
						50	51	36
$R_{j/i} = I_j/I_i$†	24·000	2·706	2·199	1·797	16·257	15·560	73·029	2·199
$R_{p/i} = I_p/I_i$‡	0·0151	0·0181	0·3109	0·448	0·056	0·8955	20·9052	0·0800
Numbering of shaft elements	9	10	11	12	13–19		20	21
	23	24	25	26	27–33		34	35
	37	38	39	40	41–47		48	49
$R_{j/i} = I_j/I_i$†	16·634	6·610	13·686	18·471	1·0		8·196	37·469
$R_{p/i} = I_p/I_i$‡	0·4412	48·379	0·1089	0·0854	0·1106		1·2306	43·783

†$R_{j/i} = I_j/I_i$ = ratio of mass moment of inertia of larger gear to that of smaller gear for each shaft element.
‡$R_{p/i} = I_p/I_i$ = ratio of mass moment of inertia of shaft to that of smaller gear for each shaft element.

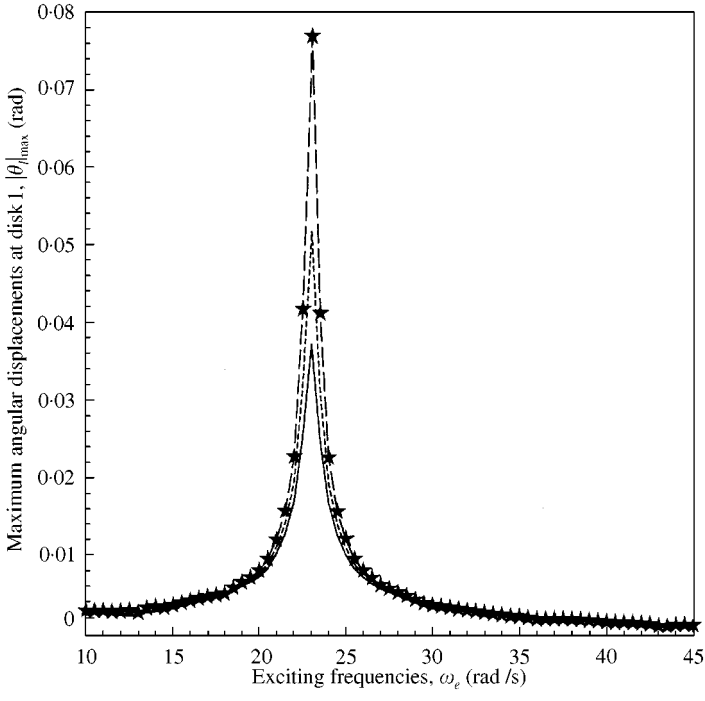

Figure 8. The frequency-response curve of disk 1 for the three-branched gear system as shown in Figure 5 due to an exciting torque $F(t) = 6000 \sin(\omega_e t)$ lb-in on disk 1: –★–, $C = 1200$ lb in s/rad; - - - - - - -, $C = 3600$ lb in s/rad; ———, $C = 6000$ lb in s/rad.

torsional angle of disk 1, $|\theta_1|_{max}$, and the exciting frequency ω_e (with time-step size $\Delta t = 0{\cdot}01$ s) is shown in Figure 8, where (- - ∗ - -) denotes the frequency-response curve for the case of the damping coefficients C_j ($j = 1$–3) = 1200 lb in sec/rad, while (- - - - -) and (——) denote those for the cases of the damping coefficients C_j ($j = 1$–3) = 3600 and

6000 lb in sec/rad respectively. From Figure 8 one sees that there exists a peak for each curve in the vicinity of $\omega_e \approx \omega_1 \approx 23{\cdot}0$ rad/s, and the peak value of $|\theta_1|_{max}$ decreases with increasing the damping coefficients C_j ($j = 1$–3). It is evident that all the above results agree with the theoretical predictions.

8. CONCLUSIONS

(1) A general formulation for the elemental property matrices (including mass matrix, damping matrix, stiffness matrix, and load vector) of a shaft element is presented. According to this formulation, the only difference between the property matrices for a shaft element connecting with the slave gear and those without connecting with the slave gear is the value of the gear (or speed) ratio of the reduction gear R_j: $R_j = r_m/r_s$ for the former and $R_j = -1{\cdot}0$ for the latter, where r_m and r_s, respectively, denote the radii of the pitch circles for the master gear and the slave gear. Since no overall transformation or element-by-element transformations are required, the presented approach is easily used to do the free or forced vibration analysis of the complicated gear-branched systems.

(2) For a torsional system composed of two rigid disks (with mass moments of inertia I_i and I_j, $I_i < I_j$) and a shaft segment with mass moment of inertia I_p, if ω_N and ω_C are the natural frequencies of the system with shaft mass (or I_p) "neglected" and "considered", respectively, then the value of $R_\omega = \omega_N/\omega_C$ is related to both the ratios of $R_{p/i} = I_p/I_i$ and $R_{j/i} = I_j/I_i$. The influence of $R_{p/i}$ on the ratio $R_\omega = \omega_N/\omega_C$ is much larger than that of $R_{j/i}$ on R_ω. In other words, the ratio of the mass moment of inertia for the shaft segment to that for the smaller disk, $R_{p/i} = I_p/I_i$, is the key parameter determining the influence on the dynamic behavior of the torsional system. The extension of the last statement is also available for the m.d.o.f. torsional system composed of more than two rigid disks and one shaft segment.

ACKNOWLEDGMENTS

The authors wish to thank the Committee of Agriculture of the Republic of China, for the financial support, and also, Dr Samuel Doughty, for his valuable comments. In addition, the authors appreciate the reviewers, for their enthusiastic citing of the grammatical mistakes throughout the paper.

REFERENCES

1. H. HOLZER 1921 *Analysis of Torsional Vibration*. Berlin: Springer.
2. W. K. WILSON 1956 and 1963 *Practical Solution of Torsional Vibration Problems*. 3rd edition, Vols. 1 & 2. London: Chapman & Hall.
3. A. H. CHURCH 1957 *Mechanical Vibration*. New York: Wiley.
4. T. W. SPAETGENS and B. C. VANCOUVER 1950 *Journal of Applied Mechanics* **17**, 59–63. Holzer method for forced-damped torsional vibrations.
5. J. P. DEN HARTOG and J. P. LI 1946 *Journal of Applied Mechanics, Transactions of ASME* **68**, 276–280. Forced torsional vibrations with damping: an extension of Holzer's method.
6. J. S. WU and W. H. CHEN 1982 *Journal of Ship Research* **26**, 176–189. Computer method for forced torsional vibration of propulsive shafting system of marine engine with or without damping.
7. L. MEIROVITCH 1967 *Analytical Methods in Vibrations*. New York: MacMillan.

8. S. DOUGHTY and G. VAFAEE 1985 *Transactions of ASME, Journal of Vibration, Acoustics, Stress and Reliability in Design* **107**, 128–132. Transfer matrix eigensolutions for damped torsional systems.
9. J. S. WU and I. H. YANG 1995 *Journal of Sound and Vibration* **180**, 417–435. Computer method for torsion-and-flexure-coupled forced vibration of shafting system with damping.
10. A. C. GILBERT 1972 *Journal of Engineering and Industrial Transactions of ASME* **94**, 279–283. A note on the calculation of torsional natural frequencies of branch systems.
11. S. SANKAR 1979 *Journal of Mechanical Design, Transactions of ASME* **101**, 546–553. On the torsional vibration of branched systems using extended transfer matrix method.
12. N. SHAIKH 1974 *Journal of Engineering and Industrial Transactions of ASME* **96**, 1006–1009. A direct method for analysis of branched torsional system.
13. B. DAWSON and M. DAVIES 1981 *The Shock and Vibration Bulletin, Bulletin* **51**, 1–10. An improvement to Shaikh's method for torsional vibration analysis of branched system.
14. P. SCHWIBINGER and R. NORDMANN 1990 *Transactions of ASME* **112**, 312–320. Torsional vibrations in turbogenerators due to network disturbances.
15. H. F. TAVARES and V. PRODONOFF 1986 *The Shock and Vibration Bulletin, Bulletin* **56**, 117–125. A new approach for gearbox modeling in finite element analyses of torsional vibration of gear-branched propulsion systems.
16. Z. S. LIU, S. H. CHEN and T. XU 1993 *Journal of Vibration and Acoustics* **115**, 277–279. Derivatives of engenvalues for torsional vibration of geared shaft systems.
17. K. J. BATHE 1982 *Finite Element Procedures in Engineering Analysis*. New Jersey: Prentice-Hall.